Thompson, D. M., Cochet, C., Chambaz, E. M., & Gill, G. N. (1985) *J. Biol. Chem. 260*, 8824–8830.
Veech, R. L., Lawson, J. W. R., Cornell, N. W., & Krebs, H. A. (1979) *J. Biol. Chem. 254*, 6538–6547.
Whitman, M., Kaplan, D. R., Schaffhausen, B., Cantley, L., & Roberts, T. M. (1985) *Nature (London) 315*, 239–341.
Whitman, M., Kaplan, D. R., Roberts, T., & Cantley, L. (1987) *Biochem. J.* (in press).

Steady-State and Time-Resolved Spectroscopic Studies on the Hematoporphyrin–Lipoprotein Complex†

Mariano Beltramini,*,‡ Patricia A. Firey,§ Fernanda Ricchelli,∥ Michael A. J. Rodgers,§ and Giulio Jori‡
Department of Biology and CNR Center for Hemocyanins and Other Metalloproteins, University of Padova, I-35131 Padova, Italy, and Center for Fast Kinetics Research, The University of Texas at Austin, Austin, Texas 78712
Received November 7, 1986; Revised Manuscript Received May 29, 1987

ABSTRACT: The interaction of hematoporphyrin (Hp) with the isolated rabbit lipoprotein fractions very low density lipoproteins, low-density lipoproteins, and high-density lipoproteins has been studied by steady-state and time-resolved spectroscopy. The porphyrin appears to be bound to both the apoprotein and the lipid phase. The two populations of lipoprotein-bound Hp molecules can be distinguished on the basis of the fluorescence excitation spectrum, decay constants of the lowest excited singlet and triplet states, and accessibility to oxygen. Upon Hp binding, the intrinsic fluorescence emission of apolipoproteins is quenched at least in part via singlet–singlet energy transfer from tryptophyl residues to the porphyrin moiety. The binding of Hp with the protein matrix can be adequately described on the basis of Scatchard analysis, whereas the interaction of Hp with the lipid core can be described as the partitioning of the dye between a hydrophobic and an aqueous phase. The Hp binding capacity of lipoproteins is maximal for very low density lipoproteins.

Plasma lipoproteins serve as an important means of transport of lipids to cells. Lipid delivery occurs after internalization of the lipoprotein particles by cells; the process takes place by two parallel compartmented routes: (i) receptor-mediated endocytosis via coated pits/coated vesicles which are degraded at the lysosome level and (ii) trapping in plasmalemmal vesicles which are taken up through the invagination of noncoated regions of cell membrane (Goldstein et al., 1979; Chapman, 1980). The receptor-mediated pathway is especially active for cells characterized by a high mitotic index, where the need for an extra supply of cholesterol and phospholipids for membrane synthesis induces the formation of a large number of low-density lipoprotein (LDL)[1] receptors on the cell surface (Devon et al., 1981; Slater et al., 1984).

These observations suggested the use of LDL as carriers of cytostatic drugs to tumor cells in vivo (Norata et al., 1984). Recently, we showed that lipoproteins play a major role in the transport of hematoporphyrin (Hp) in the bloodstream (Jori et al., 1984a) and the delivery of porphyrins to tumors in experimental animals (Jori, 1985). The specific localization of some porphyrins in neoplastic tissues is the basis of a novel modality of tumor treatment, termed photodynamic therapy (Dougherty, 1984). Significant amounts of porphyrins are also accumulated by other tissues showing cell hyperproliferation, including atheromatous plaques (Spears et al., 1983), psoriatic areas (Berns et al., 1984), and metastatic abscesses (Venezio et al., 1985).

Therefore, it appears of interest to characterize the complexes of Hp with the most important classes of serum lipoproteins, namely, VLDL, LDL, and HDL. We have studied the Hp–lipoprotein system by means of steady-state and time-resolved emission spectroscopy, which is very sensitive to the nature of the Hp microenvironment (Jori & Spikes, 1984). Our studies have been centered on those lipoprotein fractions which can be isolated by standard sequential density flotation; hence, they are not intended to define the detailed binding mode of Hp with specific sites; rather, they describe the properties of the complexes between Hp and systems, though heterogeneous, which are important for its transport and tissue delivery in vivo.

Materials and Methods

Hematoporphyrin. Hp was purchased from Porphyrin Products (Logan, UT). Analysis of the sample by high-pressure liquid chromatography showed the presence of about 12% impurities including protoporphyrin IX (3–4%), [(hydroxyethyl)vinyl]deuteroporphyrin IX (5%), and some highly aggregated material.

The concentration of Hp aqueous solutions was determined spectrophotometrically using the molar extinction coefficient $\epsilon = 4.23 \times 10^5\ M^{-1}\ cm^{-1}$ at 401 nm in 1 M HCl (Marks, 1969).

† Time-resolved experiments were performed at the Center for Fast Kinetics Research (CFKR) at The University of Texas at Austin. The CFKR is supported jointly by NIH Grant RR00886 from the Biomedical Research Technology Program of the Division of Research Resources and by The University of Texas at Austin. Partial support for this project came from NIH Grant GM24235 (M.A.J.R.). This work was supported in part by Consiglio Nazionale delle Ricerche (Italy) under the special project "Oncologia", Contract 85.02205.44 115.05970.
* Address correspondence to this author at the Department of Biology, University of Padova.
‡ Department of Biology, University of Padova.
§ Center for Fast Kinetics Research, The University of Texas at Austin.
∥ CNR Center for Hemocyanins and Other Metalloproteins, University of Padova.

[1] Abbreviations: LDL, low-density lipoprotein(s); VLDL, very low density lipoprotein(s); HDL, high-density lipoprotein(s); Hp, hematoporphyrin IX; SDS, sodium dodecyl sulfate; HSA, human serum albumin.

0006-2960/87/0426-6852$01.50/0

Table I: Average Composition (%) of Lipoproteins[a]

	VLDL	LDL	HDL
protein	13	33	56
triglycerides	48	28	13
total cholesterol[b]	5	21	9
phospholipids	34	18	22

[a] Data refer to an average of six preparations. Data are expressed as the percentage of total weight of the lipoprotein. For details on chemical determinations, see Materials and Methods. [b] Total cholesterol refers to the sum of free and esterified cholesterol.

Preparation and Characterization of Lipoproteins. Lipoproteins were isolated from rabbit serum. New Zealand white rabbits were supplied by Ditta Conigli and C., Padova (Italy), and were kept on a standard diet, allowing free access to food and tap water. Blood samples (approximately 30 mL) were taken from the ear artery of the rabbit previously fasted for 12 h. Rabbit blood was clotted at room temperature for 30 min and subsequently centrifuged at 3000 rpm for 15 min. Lipoproteins were fractioned from the serum by sequential density flotation according to Havel et al. (1955), using a Beckman L 5-65 preparative ultracentrifuge with a Beckman 40.3 rotor. Three fractions were isolated, namely, VLDL ($d \leq 1.006$ g/mL), LDL (1.006 g/mL $\leq d \leq$ 1.063 g/mL), and HDL (1.063 g/mL $\leq d \leq$ 1.21 g/mL). Lipoprotein flotation was accomplished at the different densities by centrifuging the serum at 39000 rpm for 18 h. After separation of each fraction, the serum density was adjusted to the desired value (1.063 and 1.21 g/mL, respectively, for LDL and HDL) by adding either an aliquot of a 1.335 g/mL KBr solution (to 1.063 g/mL) or solid KBr (to 1.21 g/mL). Each separated fraction was further purified by a second ultracentrifugation at the appropriate density. The VLDL fraction was isolated at the physiological density of plasma (d = 1.006 g/mL). Purified lipoproteins were then dialyzed exhaustively against 10 mM phosphate buffer, pH 7.0, containing 150 mM NaCl. All operations were carried out at 4 °C. The purity of each lipoprotein fraction was assayed by agarose gel electrophoresis (Noble, 1968).

In order to calculate the lipoprotein concentration, each fraction was analyzed for the content of apoproteins (Lowry et al., 1961), total cholesterol (free plus esterified) (Roeschlau, 1974), triglycerides (Wahlefeld, 1976), and phospholipids (Zilversmit, 1950). The lipoprotein concentration (in milligrams per milliliter) was calculated as the sum of the concentrations of the different components. The average composition of our preparations (in percent) is reported in Table I.

The Hp–lipoprotein complex was prepared by direct addition of suitable amounts of an Hp solution (final concentration ranged between 2 and 90 μM) to each lipoprotein fraction (approximately 0.3 mg/mL) at room temperature, followed by dialysis against 10 mM phosphate buffer, pH 7.4, containing 150 mM NaCl at 4 °C.

Steady-State Spectroscopic Measurements. Absorption spectra were recorded at room temperature with a Perkin-Elmer 576 spectrophotometer.

Fluorescence spectra were determined at 21 ± 0.1 °C with a Perkin-Elmer MPF 4 spectrophotofluorometer operating in the "ratio" mode in order to minimize errors due to fluctuations of the light source. The spectra were corrected for the inner filter effect by using the multiplicative correction factor (Chignell, 1972):

$$X = \text{antilog}\left(\frac{A_{exc} + A_{em}}{2}\right) \quad (1)$$

where A_{exc} and A_{em} indicate the absorbancies of the sample at the excitation and emission wavelengths, respectively. No correction was applied for the wavelength dependence of the photomultiplier response.

Fluorescence polarization spectra of lipoprotein-bound Hp were recorded (λ_{exc} = 440 nm) with a Hitachi polarizer–analyzer system inserted into the Perkin-Elmer spectrophotofluorometer. Fluorescence polarization, $P(\lambda)$, was calculated by using the expression:

$$P(\lambda) = (I_{\parallel} - I_{\perp})/(I_{\parallel} + I_{\perp}) \quad (2)$$

where $I_{\parallel}$ and $I_{\perp}$ are emitted intensities parallel and perpendicular to the linearly polarized exciting light, respectively. The values of $P(\lambda)$ were corrected for instrumental artifacts by the methods of Azumi and Mc Glynn (1962).

The binding of Hp to lipoproteins was studied by using the Scatchard equation (Scatchard, 1949):

$$\bar{\nu}/c = nK_A - \bar{\nu}K_A \quad (3)$$

where $\bar{\nu}$ (in nanomoles per milligram) is the ratio of bound Hp to lipoproteins, c (in nanomoles per milliliter) is the concentration of free Hp (total Hp added minus bound Hp), and K_A (in M^{-1}) is the association constant of the Hp–lipoprotein complex. Since lipoprotein complexes contain several apolipoproteins whose molecular weights range from approximately 6500 to 250000 (Ganesan et al., 1975; La Rosa et al., 1970), it is not possible to calculate n as the number of Hp binding sites per mole of lipoprotein. In our calculations, n refers to the number of nanomoles of Hp bound per milligram of protein. To 1 mL of each lipoprotein fraction in phosphate buffer, suitable aliquots of a stock aqueous Hp solution were added up to a final Hp concentration of about 60 μM. Experiments were performed at 21 ± 0.1 °C using four different concentrations of each lipoprotein fraction. The titrations were carried out spectrophotofluorometrically following both the decrease of lipoprotein intrinsic fluorescence (λ_{exc} = 295 nm, emission 300–450 nm) and the increase of Hp fluorescence (λ_{exc} = 440 nm, emission 550–780 nm). In the first case, the concentration of bound Hp was calculated according to Beaven et al. (1974) [see also Halfman and Nishida (1972)], and the data referred to the apolipoprotein concentration; in the second case, the amount of bound Hp was calculated according to Azzi (1974), while the data referred to the total lipoprotein mass.

Time-Resolved Spectroscopic Measurements. Fluorescence lifetimes were measured at 21 °C by using the time-correlated single-photon counting method. A cavity-dumped (800 kHz) pulsed dye laser was the excitation source (Rhodamine 6G tuned to 578 nm). This was synchronously pumped by a mode-locked (82 MHz), frequency-doubled (532 nm) Nd:YAG continuous-wave laser. Total fluorescence was collected either above 630 nm by the use of cutoff filters or at different wavelengths using a monochromator with slit widths at 3 nm. The system and its characteristics have been previously described (Rodgers & Firey, 1985).

Triplet lifetimes were measured at 21 °C with a system similar to that described by Reddi et al. (1983). A Q-switched Nd:YAG pulsed laser (12-ns duration) system operating at 532 nm (ca. 150 mJ/pulse) was the excitation source.

Fitting of decay profiles was accomplished with an iterative nonlinear least-squares routine using the CFKR's dedicated PDP 1170 computer array (Rodgers & Firey, 1985).

Results

Steady-State Absorption and Fluorescence Studies. Incubation of 9 μM Hp with the isolated lipoprotein fractions

Table II: Kinetic Parameters of the First Excited Singlet (S_1) and Triplet (T_1) States of Lipoprotein-Bound Hematoporphyrin

parameter	VLDL		LDL	
	fast[c]	slow[c]	fast[c]	slow[c]
S_1 decay constant[a]	18.0 (37)	5.6 (63)	48.0 (58)	8.0 (42)
T_1 decay (N_2) constant[a]	3.2 (44)	0.5 (56)	1.5 (55)	0.2 (45)
bimolecular oxygen quenching rate constant[b]	1.0 (27)	0.4 (73)	1.2 (58)	0.5 (42)

[a] Values in $s^{-1} \times 10^{-4}$ for T_1 and $s^{-1} \times 10^{-7}$ for S_1. [b] Values in $M^{-1} s^{-1} \times 10^{-9}$ calculated by taking $[O_2] = 0.28$ mM in air-equilibrated aqueous buffer at room temperature. [c] The numbers in parentheses indicate the percent weight of each component.

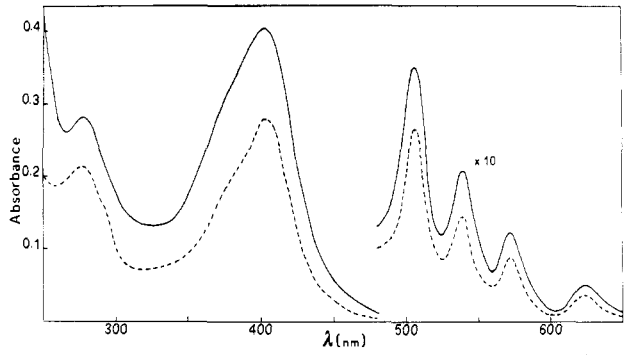

FIGURE 1: Absorption spectra of LDL-bound Hp (solid line) and HDL-bound Hp (dashed line). LDL (0.38 mg/mL) was incubated with 9.1 μM Hp. HDL (0.322 mg/mL) was incubated with 4.2 μM Hp. Excess Hp was removed as described under Materials and Methods.

causes a shift of the porphyrin absorption maximum in the Soret region from about 370 to 405 nm; the absorption spectrum in the near-UV and visible region of the exhaustively dialyzed Hp–LDL and –HDL systems is shown in Figure 1. A similar absorption spectrum is obtained for the Hp–VLDL system, although the marked contribution of light scattering induces some distortion of the spectral features. The position of the Soret maximum and the width of the band are typical of monomeric Hp (Jori & Spikes, 1984). Moreover, the four-band pattern in the 500–630-nm region typical of the porphyrin chromophore (Corwin, 1973) is preserved after Hp binding to lipoproteins.

As shown in Figure 2, binding of Hp to LDL also leads to about a 20-nm bathochromic shift of the fluorescence maximum; the flattening of the spectrum between the 632- and 697-nm bands probably reflects the onset of a new emission centered around 660 nm. Similar fluorescence emission spectra were obtained for the complexes of Hp with VLDL and HDL (data not shown).

Indications that the population of lipoprotein-bound Hp is heterogeneous are obtained by fluorescence excitation spectra. For all the Hp–lipoprotein complexes, the position of the excitation maximum in the Soret region is dependent on the emission wavelength (Figure 3): in particular, the fluorescence bands peaking at 632 and 687 nm have an excitation maximum at 400 nm, while the excitation of the fluorescence emitted between 640 and 660 nm has a maximum at 410 nm. The fluorescence excitation spectrum of Hp in aqueous solution is independent of the emission wavelength.

The fluorescence emitted by lipoprotein-bound Hp exhibits a significant degree of polarization (Figure 4) especially for the Hp–VLDL system. The fluorescence emission of Hp in aqueous solution is devoid of any significant polarization (Srivastava et al., 1973).

Time-Resolved Emission Studies. The decay plots of the lowest excited singlet (S_1) and triplet (T_1) states of lipoprotein-bound Hp are satisfactorily fitted by two first-order exponential functions; this suggests the existence of at least two species. The decay rate constants and the relative weights

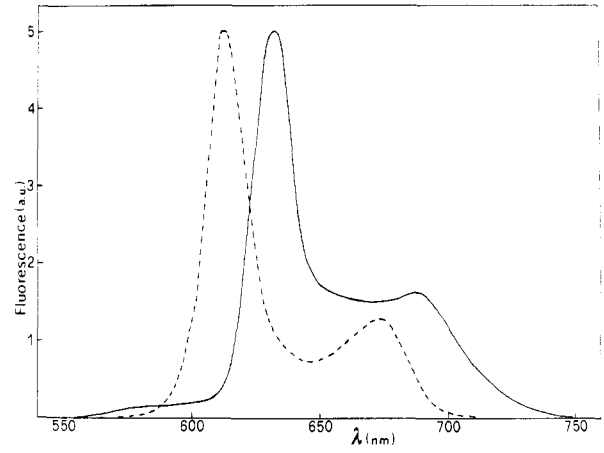

FIGURE 2: Emission spectra of LDL-bound Hp (solid line) and free Hp (0.4 μM) in phosphate buffer (dashed line). Conditions as described in Figure 1. The two emission spectra (λ_{exc} = 440 nm) were normalized to the same intensity at the emission maxima.

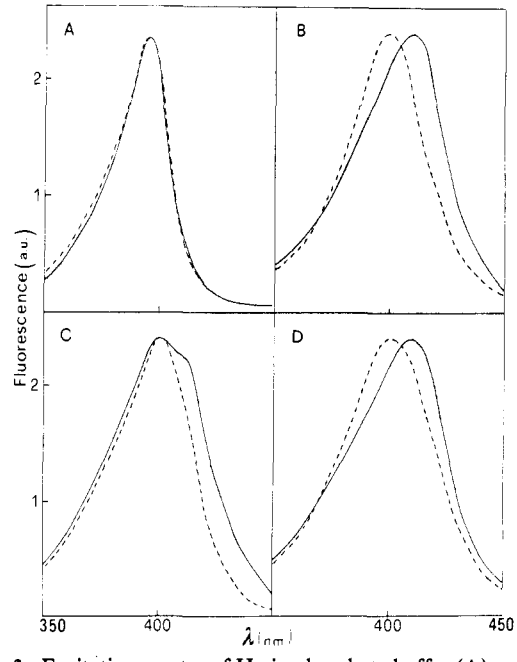

FIGURE 3: Excitation spectra of Hp in phosphate buffer (A) or bound to VLDL (B), LDL (C), and HDL (D). Emission λ at 640 nm (solid lines) and 615 nm (dashed lines). The spectra are corrected for the inner filter effects and normalized to the same fluorescence intensity at the excitation maxima. For details, see Materials and Methods.

of each component from extrapolations to zero time for the VLDL and LDL systems are reported in Table II. The order of magnitude of the decay constants is comparable with that of Hp incorporated into SDS micelles or unilamellar liposomes of dipalmitoylphosphatidylcholine (Rodgers, 1985). The relative percentages of the lifetime components of the fluorescence decay are presented as a function of emission wavelength in Table III. At each wavelength, two components, fast and slow, are still evident with lifetimes independent

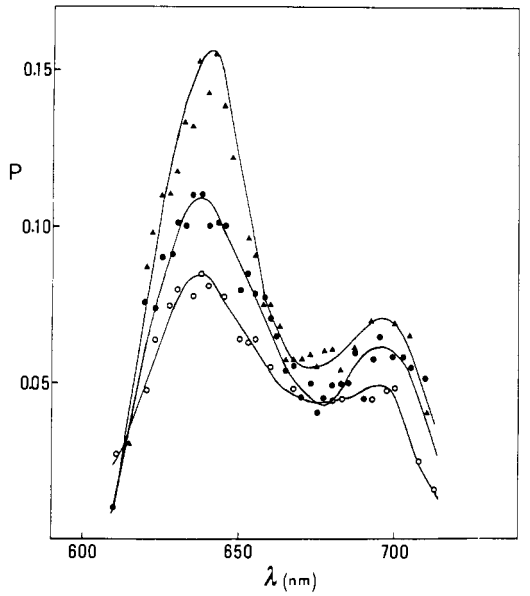

FIGURE 4: Fluorescence polarization spectra of Hp bound to VLDL (▲), LDL (○), and HDL (●). Excitation λ at 440 nm. For details, see Materials and Methods.

Table III: Emission Wavelength Resolved Fluorescence Lifetime Components of LDL-Bound Hp[a]

	relative weight	
wavelength (nm)	fast component	slow component
620	50	50
630	49	51
640	65	35
650	74	26
660	73	27
670	71	29
680	57	43

[a] Relative weights were expressed as relative percentages of total counts. Total counts for each determination were 7×10^3.

of emission wavelength. However, the relative weight of the fast component significantly changes, reaching a maximum between 650 and 670 nm. This wavelength range agrees with the location of the emission peak at 660 nm.

The T_1 state of lipoprotein-bound Hp is collisionally quenched by oxygen. Thus, the triplet lifetime of VLDL-complexed Hp decreases from 31 and 204 μs (fast- and slow-decaying components) to 3.2 and 8.5 μs, respectively, in N_2-saturated and air-equilibrated aqueous solutions. For LDL-complexed Hp, the T_1 lifetimes of the fast- and slow-decaying triplets in air-equilibrated solutions are 2.8 and 5.3 μs, respectively, as compared with the corresponding 68- and 435-μs lifetimes in deaerated systems. The bimolecular rate constants for the quenching of Hp(T_1) by oxygen (k_{O_2}) are approximately 2-fold larger for the fast than for the slow component in both VLDL- and LDL-Hp complexes (Table II). The k_{O_2} values are consistent with a diffusion-limited process, in agreement with the ready diffusibility of oxygen across lipid/water and lipid/protein interphases (Lindig & Rodgers, 1981).

Quenching of the Intrinsic Lipoprotein Fluorescence by Bound Hp. Upon 295-nm excitation, the three lipoprotein fractions give the typical fluorescence emission of tryptophyl residues peaking at about 330 nm. The intensity of the intrinsic fluorescence is strongly affected by Hp binding. In Figure 5, we show the dependence of the F/F^0 ratio (where F and F^0 are the fluorescence intensities in the presence and absence of bound Hp, respectively) on the absorbance of bound Hp at 405 nm. In all cases, one can notice a rapid decrease

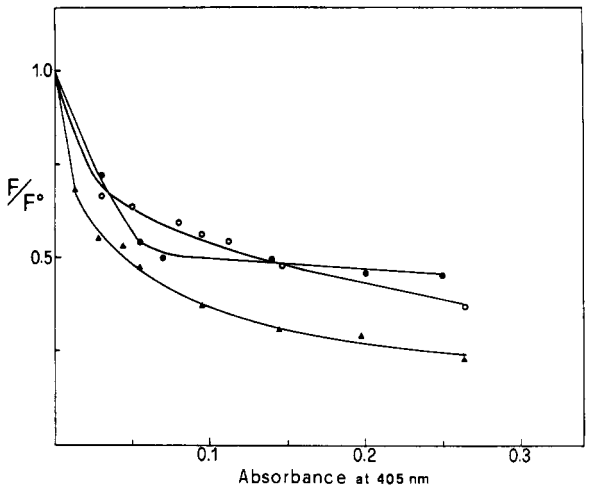

FIGURE 5: Quenching of lipoprotein intrinsic fluorescence induced by Hp binding. The fluorescence intensity at 330 nm (λ_{exc} = 295 nm) is plotted vs. the absorbance at 405 nm. The data refer to VLDL (●), LDL (○), and HDL (▲). Fluorescence intensities are normalized to the same absorbance at the excitation λ. F^0 and F are the fluorescence intensities at 330 nm in the absence and in the presence of bound Hp, respectively.

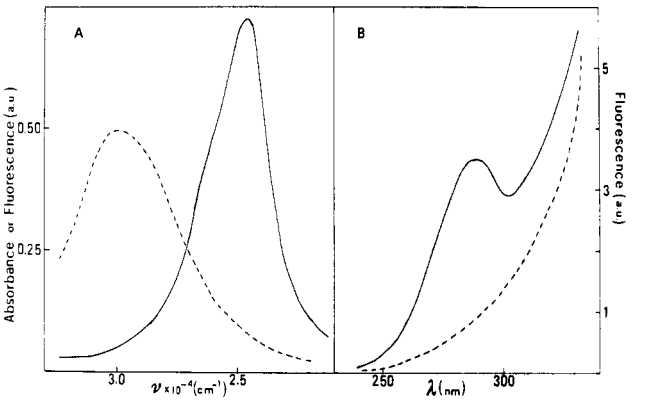

FIGURE 6: Singlet–singlet tryptophan–Hp energy transfer. (A) Fluorescence emission spectrum of HDL tryptophan (λ_{exc} = 295 nm) in the absence of bound Hp (dashed line) and absorption spectrum of HDL-bound Hp corrected for lipoprotein absorption (solid line). (B) Excitation spectra of free (dashed line) and HDL-bound Hp (solid line). Emission λ at 620 nm.

of F/F^0 in the presence of relatively low amounts of bound Hp. The observed effect can be attributed, at least in part, to singlet–singlet energy transfer from protein tryptophyl residues to bound Hp. As shown in Figure 6A, there is a significant overlap between the emission spectrum of tryptophan and the absorption spectrum of Hp. Furthermore, the excitation spectrum of the fluorescence emitted by bound Hp at 630 nm shows a peak around 290 nm, which corresponds with the excitation maximum of tryptophan fluorescence (Figure 6B). Free Hp displays no fluorescence excitation band below 300 nm.

Analysis of Hp Binding by Lipoproteins. The binding of Hp by lipoproteins has been studied by the Scatchard method (Scatchard, 1949), and the experimental data were analyzed according to eq. 3. Different plots are obtained depending on whether one studies the binding process by following the fluorescence emitted by Hp (Figure 7) or the quenching of the intrinsic lipoprotein fluorescence (Figure 8A,B). In particular, biphasic plots are observed for Hp fluorescence while the tryptophan quenching data are fitted by a single straight line. From the linear portion of the plots of Figure 7 and the straight lines of Figure 8, one can estimate n and K_A values (see Table IV). The n values, calculated from

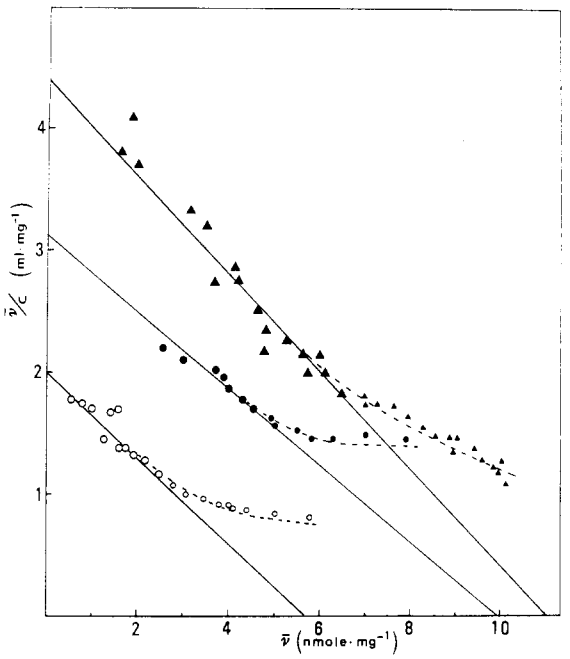

FIGURE 7: Binding of Hp to lipoproteins. Scatchard plots obtained by following the changes of Hp fluorescence at 630 nm (λ_{exc} = 440 nm) in the presence of VLDL (▲), LDL (○), and HDL (●). Conditions are given in the text.

Table IV: Binding Parameters of Hp to Lipoproteins[a]

protein	$K_A \times 10^{-6}$ [b]	n[b]	$K_A \times 10^{-6}$ [c]	n[c]
VLDL	1.16	55	0.40	50
LDL	0.70	21	0.35	19
HDL	0.60	19	0.31	20

[a] $K_A \times 10^{-6}$ are expressed as M^{-1} and n as μmol·g^{-1}. [b] Values are calculated from the Scatchard plots of Figure 8 obtained by following the quenching of the lipoprotein intrinsic fluorescence. [c] Values are calculated from the Scatchard plots of Figure 7 obtained by following the fluorescence emitted by bound Hp. In this latter case, the n values were normalized to an apoprotein content of 100%. In these experiments, the apoprotein content was 22% for VLDL, 30% for LDL, and 49% for HDL.

Figure 7 for the different lipoprotein classes, were normalized to the same apoprotein content.

Discussion

Lipoproteins are currently viewed as high molecular weight particles in which a surface layer of protein and amphiphilic lipid molecules encapsulates a nonpolar core of triglyceride and esterified cholesterol molecules. As a consequence, aqueous solutions of lipoproteins allow the partition of relatively water-soluble hydrophobic molecules between two phases of different polarity. Hp can be expected to interact readily with lipoproteins owing to its n-octanol/water partition coefficient of about 8 (Jori & Spikes, 1984) and its incorporation into the phospholipid bilayer of liposomes (Ricchelli & Jori, 1985).

The spectroscopic properties of Hp bound with the three lipoprotein fractions are typical of porphyrin molecules in a hydrophobic microenvironment. Thus, the bathochromic shift of the absorption and fluorescence emission maxima has been observed for monomerization of Hp and/or solubilization of the dye in nonpolar media (Kessel & Rossi, 1983). The location of Hp molecules in the lipid core of lipoproteins is further supported by the appearance of an emission feature at about 660 nm, similar to that observed for Hp associated with unilamellar vesicles of dipalmitoylphosphatidylcholine (Jori et al., 1984b). Due to the large heterogeneity of lipo-

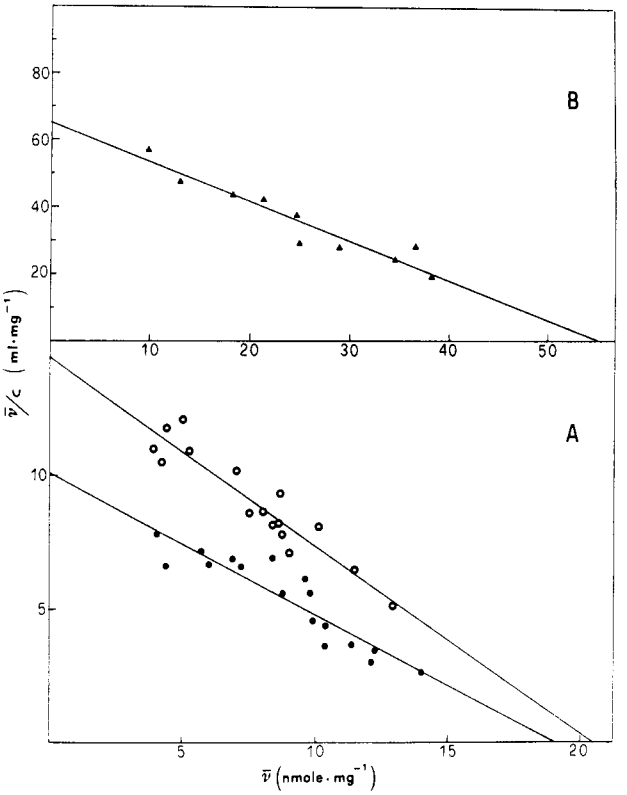

FIGURE 8: Binding of Hp to lipoproteins. Scatchard plots obtained by following the changes of lipoprotein intrinsic fluorescence at 330 nm (λ_{exc} = 295 nm). Experimental points obtained for (A) LDL (○) and HDL (●) and (B) VLDL (▲).

protein fractions, Hp molecules are probably distributed among areas with different physicochemical properties. Therefore, at the present stage of our investigations, the spectroscopic data are likely to represent an average of the different situations. A typical example is given by fluorescence polarization spectra of Hp bound with the three lipoprotein fractions (Figure 4). Indeed, the mobility of Hp is restricted in all lipoproteins, although no clear correlation is found between the degree of polarization and the lipid or protein content of the single fractions.

The spectroscopic properties reported in this paper are consistent with a heterogeneous distribution of Hp molecules in the lipoproteins matrix: the fluorescence excitation maximum changes as a function of the emission wavelength. Moreover, both the S_1 and T_1 states of lipoprotein-bound Hp decay biphasically, and the relative percentages of each fluorescent component change as a function of the emission wavelengths as well. A similar two-component decay was observed for Hp in aqueous solution and has been ascribed to aggregated and monomeric forms of the dye (Rodgers, 1985). However, our steady-state spectroscopic studies indicate the presence only of monomeric Hp in lipoproteins; hence, the short- and fast-decaying Hp species are likely to be located in different compartments within the lipoproteins matrix. The same line of evidence is provided by the different bimolecular rate constants found for the quenching of two populations of Hp(T_1) by oxygen. One population appears to be readily accessible to O_2 as shown by the $k_{O_2} \sim 10^9$ M^{-1} s^{-1} similar to that obtained for O_2 quenching of Hp in micellar systems; the second population is more shielded, k_{O_2} being 1 order of magnitude lower ($\sim 10^8$ M^{-1} s^{-1}) as it has been previously observed for HSA-bound Hp (Reddi et al., 1984).

The Scatchard plots in Figure 7 indicate a two-step interaction of Hp with lipoproteins. The initial portion of the plots

reflects the interaction of the dye with a discrete set of sites of comparable affinity, which appear to be located in the protein moiety of lipoproteins; as shown in Figure 6, there is energy transfer between lipoprotein tryptophyl residues and bound Hp. This process strongly depends on the mutual distance and orientation of the donor and acceptor species, and its efficiency decays as a function of the sixth power of the distance (Förster, 1959). Energy transfer might also occur from tryptophan to Hp molecules at the lipid–protein interphase; however, in this case, a nonlinear Scatchard plot would be expected by following the quenching of tryptophan fluorescence. In agreement with our hypothesis, the K_A calculated from the Scatchard plots describing the binding of Hp to the high-affinity sites (Figure 7) and the quenching of tryptophan fluorescence (Figure 8) are comparable (see Table IV) provided one takes into account that the K_A's obtained in Figure 7 are artificially lowered due to the influence of the second portion of the plots. Indeed, the number of high-affinity binding sites, obtained by the two types of Scatchard plots, are very similar (Table IV). Our K_A values are in good agreement with the K_A value reported by Reyftmann et al. (1984) on the binding of Hp of human LDL, as measured by equilibrium dialysis ($K_A = 0.86 \times 10^6$ M^{-1}).

Only a limited number of bound Hp molecules causes the quenching of tryptophan fluorescence, as shown by the decrease in the slope of the quenching curves beyond a given value of absorbance of bound Hp (Figure 5). The additionally bound Hp is associated with a very high number of low-affinity sites as suggested by the small slope of the second portion of the Scatchard plots (Figure 7). This pool of Hp should be partitioned in the lipid phase of lipoproteins, which includes a variety of both neutral and polar lipid regions. The latter class of lipid sites is likely to be responsible for the binding of Hp with HDL.

It is interesting to note that the spectroscopic properties of the various Hp–lipoprotein complexes, the parameters describing Hp binding with the various lipoprotein fractions, and the accessibility of Hp to O_2 (Table II) are very similar for LDL and VLDL, in spite of the large differences in the lipid content/composition and the relative abundance of the various apoproteins (Morrisett et al., 1975). These observations strongly argue for a Hp–lipoprotein complexation occurring via both phase partitioning of the dye within the lipid moiety and apoprotein interaction. The capability of lipoproteins to bind large amounts of Hp is in agreement with earlier observations on the binding of cholesterol to HDL (Lund-Katz et al., 1984). HDL have been found to solubilize in vitro significant amounts of extra cholesterol, indicating that the lipoprotein molecule is not saturated with the lipid under normal physiological conditions.

These data are relevant to the interpretation of the mechanisms controlling the transport of porphyrins and their delivery to normal and tumor tissues. Recent pharmacokinetic studies (Jori, 1985) indicated that LDL and their metabolic precursors, VLDL, play a key role in the preferential delivery of Hp to rapidly proliferating cells, including neoplastic cells. On the other hand, HDL are responsible for the prolonged persistence of Hp in the serum, hence for the general photosensitivity displayed by patients treated with Hp (Zalar et al., 1977). The findings described in this paper indicate that the different distribution and clearance of Hp bound with the various lipoproteins do not reflect a difference in the stability and structure of the complexes. Recent studies (Barel et al., 1986) show that the in vitro prepared LDL–Hp complex is stable when injected into rabbits; indeed, less than 10% of total LDL-bound Hp is transferred to other lipoproteins within 12 h from injection. Therefore, the preferential uptake of Hp by tumor cells appears to be the consequence of the pathway of LDL–cell interaction and not an intrinsic property of the drug. Furthermore, the high binding capacity of LDL for Hp in the lipid moiety makes this plasma component an efficient and specific vector for photodynamic therapy. A more refined understanding of the modalities by which lipoproteins transport and deliver associated drugs in vivo should open new prospects for the treatment of diseases characterized by an abnormally high mitotic index of the cells.

Registry No. Hp, 14459-29-1; Trp, 73-22-3; O_2, 7782-44-7; cholesterol, 57-88-5.

REFERENCES

Azumi, T., & Mc Glynn, S. P. (1962) *J. Chem. Phys. 37*, 2413.

Azzi, A. (1974) *Methods Enzymol. 32*, 234.

Barel, A., Jori, G., Perin, A., Romandini, P., Pagnan, A., & Biffanti, S. (1986) *Cancer Lett. 32*, 145.

Beaven, G. H., Chen, S. H., D'Albis, A., & Gratzer, W. B. (1974) *Eur. J. Biochem. 41*, 539.

Berns, M. W., Rettenmaier, M., Mc Cullough, J., Coffey, J., Wile, A., Disaia, P., & Weinstein, G. (1984) *Lasers Surg. Med. 4*, 73.

Chapman, M. J. (1980) *J. Lipid Res. 21*, 789.

Chignell, C. F. (1972) *Methods Pharmacol. 2*, 33.

Corwin, A. H. (1973) *Ann. N.Y. Acad. Sci. 206*, 201.

Dougherty, T. J. (1984) *Urology (Suppl.) 23*, 61.

Devon, C. A., Attie, A. D., Pangburn, S. H., & Steinberg, D. (1981) *J. Lipid Res. 22*, 37.

Förster, T. (1959) *Discuss. Faraday Soc. No. 27*, 7.

Ganesan, D., Bradford, R. H., Ganesan, G., Mc Conathy, W. J., Alaupovic, P., & Bass, H. B. (1975) *J. Appl. Physiol. 39*, 1022.

Goldstein, J. L., Anderson, R. G. W., & Brown, M. S. (1979) *Nature (London) 279*, 679.

Halfman, C. J., & Nishida, T. (1972) *Biochemistry 11*, 3493.

Havel, R. J., Eder, H. A., & Bragdon, J. H. (1965) *J. Clin. Invest. 34*, 1345.

Jori, G. (1985) in *Photodynamic Therapy of Tumors and Other Diseases* (Jori, G., & Perria, C. A., Eds.) p 159, Libreria Progetto Editore, Padova, Italy.

Jori, G., & Spikes, J. D. (1984) in *Topics in Photomedicine* (Smith, K. C., Ed.) p 183, Plenum Press, New York.

Jori, G., Beltramini, M., Reddi, E., Salvato, B., Pagnan, A., & Ziron, L. (1984a) *Cancer Lett. 24*, 291.

Jori, G., Garbo, G. M., Reddi, E., & Cozzani, I. (1984b) *Med., Biol., Environ. 12*, 291.

Kessel, D., & Rossi, E. (1982) *Photochem. Photobiol. 35*, 37.

La Rosa, J. C., Levy, R. I., Herbert, P., Lux, S. E., & Fredrickson, D. S. (1970) *Biochem. Biophys. Res. Commun. 41*, 57.

Lindig, B. A. & Rodgers, M. A. J. (1981) *Photochem. Photobiol. 33*, 627.

Lowry, O. H., Rosebrough, M. J., Farr, A. L., & Randall, R. J. (1961) *J. Biol. Chem. 193*, 265.

Lund-Katz, S., & Phillips, M. C. (1984) *Biochemistry 23*, 1130.

Marks, G. S. (1969) in *Heme and Chlorophyll*, p 169, Van Nostrand, London.

Morrisett, J. D., Jackson, R. L., & Gotto, A. M., Jr. (1975) *Annu. Rev. Biochem. 44*, 183.

Noble, R. P. (1968) *J. Lipid Res. 9*, 693.

Norata, G., Canti, G., Ricci, L., Nicolin, A., Trezzi, E., & Catapano, A. L. (1984) *Cancer Lett. 25*, 203.

Reddi, E., Jori, G., Rodgers, M. A. J., & Spikes, J. D. (1983) *Photochem. Photobiol. 38*, 639.
Reddi, E., Roders, M. A. J., & Jori, G. (1984) in *Porphyrin Localization and Treatment of Tumors* (Doiron, D. R., & Gomer, C. J., Eds.) p 373, Alan R. Liss, New York.
Reyftmann, J. P., Morliere, P., Goldstein, S., Santus, R., Dubertret, L., & Lagrange, D. (1984) *Photochem. Photobiol. 40*, 721.
Ricchelli, F., & Jori, G. (1985) in *Photodynamic Therapy of Tumors and Other Diseases* (Jori, G., & Perria, C., Eds.) p 85, Libreria Progetto Editore, Padova, Italy.
Rodgers, M. A. J. (1985) in *Photodynamic Therapy of Tumors and Other Diseases* (Jori, G., & Perria, C., Eds.) p 21, Libreria Progetto Editore, Padova, Italy.
Rodgers, M. A. J., & Firey, P. A. (1985) *Photochem. Photobiol. 42*, 613.
Roeschlau, P. (1974) *Z. Klin. Chem. Klin. Biochem. 12*, 403.
Scatchard, G. (1949) *Ann. N.Y. Acad. Sci. 51*, 660.
Slater, H. R., Mc Kinney, L., Packard, C. J., & Sheperd, J. (1984) *Arteriosclerosis (Dallas) 4*, 604.
Spears, J. R., Serur, J., Shropshire, D., & Paulin, S. (1983) *J. Clin. Invest. 71*, 395.
Srivastava, R. C., Anand, V. D., & Carper, W. R. (1973) *Appl. Spectrosc. 27*, 444.
Venezio, F. R., Divincenzo, C., Sherman, D., Reichman, M., Origitano, T. C., Thompson, K., & Reichman, O. H. (1985) *J. Infect. Dis. 151*, 166.
Wahlefeld, A. W. (1976) in *Methods of Enzymatic Analysis* (Bergmeyer, H. V., Ed.) 2nd ed, p 1831, Academic Press, New York and London.
Zalar, G. L., Poh-Fitzpatrick, M., Krohn, D. L., Jacobs, R. & Harber, L. C. (1977) *Arch. Dermatol. 113*, 1392.
Zilversmit, D. B., & Davis, A. K. (1950) *J. Lab. Clin. Med. 35*, 155.

2-[(4-Bromo-2,3-dioxobutyl)thio]- and 2-[(3-Bromo-2-oxopropyl)thio]adenosine 2′,5′-Bisphosphate: New Nucleotide Analogues That Act as Affinity Labels of Nicotinamide Adenine Dinucleotide Phosphate Specific Isocitrate Dehydrogenase†

Jerome M. Bailey and Roberta F. Colman*
Department of Chemistry and Biochemistry, University of Delaware, Newark, Delaware 19716
Received March 17, 1987; Revised Manuscript Received June 10, 1987

ABSTRACT: Two new reactive adenine nucleotide analogues have been synthesized and characterized: 2-[(4-bromo-2,3-dioxobutyl)thio]adenosine 2′,5′-bisphosphate (2-BDB-TA-2′,5′-DP) and 2-[(3-bromo-2-oxopropyl)thio]adenosine 2′,5′-bisphosphate (2-BOP-TA-2′,5′-DP). Starting with $NADP^+$, 2′-phosphoadenosine 5′-(diphosphoribose) (PADPR) was generated enzymatically and was converted to PADPR 1-oxide by reaction with *m*-chloroperoxybenzoic acid. Treatment with NaOH followed by reaction with carbon disulfide yielded 2-thioadenosine 2′,5′-bisphosphate (TA-2′,5′-DP). Condensation of TA-2′,5′-DP with 1,4-dibromobutanedione or 1,3-dibromo-2-propanone gave the final products 2-BDB-TA-2′,5′-DP and 2-BOP-TA-2′,5′-DP, respectively. The structure of these new reagents was determined by UV, ^1H NMR, ^{31}P NMR, and ^{13}C NMR spectroscopy as well as by bromide and phosphorus analysis. Both of these reagents exhibit properties expected for an affinity label of the coenzyme site of $NADP^+$-dependent isocitrate dehydrogenase. With both reagents, biphasic kinetics of inactivation are observed that can be described in terms of a fast initial phase of inactivation resulting in partially active enzyme of 6–7% residual activity, followed by a slower phase leading to total inactivation. The inactivation rate constants for both reagents exhibit a nonlinear dependence on reagent concentration, consistent with the formation of a reversible complex with the enzyme prior to irreversible modification. The enzyme incorporates both reagents to a limited extent and is protected against inactivation by $NADP^+$ and NADPH. The reaction of these new nucleotide analogues with isocitrate dehydrogenase is compared to the much slower inactivation caused by bromoacetone, indicating the importance of the nucleotide moiety in the functioning of the affinity labels. It is likely that 2-BDB-TA-2′,5′-DP and 2-BOP-TA-2′,5′-DP will have general applicability as affinity labels for other $NADP^+$ binding enzymes.

Pig heart $NADP^+$-dependent isocitrate dehydrogenase [*threo*-D_s-isocitrate:$NADP^+$ oxidoreductase (decarboxylating), EC 1.1.1.42] catalyzes the oxidative decarboxylation of isocitrate. Extensive chemical modification studies have been performed with isocitrate dehydrogenase by using a variety of group-specific reagents [see Colman (1983a) for a review]. The technique of affinity labeling, using nucleotide analogues with reactive functional groups, can potentially result in more specific chemical modification and should allow the identification of critical amino acid residues within the nucleotide binding site (Colman, 1983b). Studies of the binding of coenzymes and coenzyme fragments to $NADP^+$-specific isocitrate dehydrogenase have demonstrated that a 2′-phosphate is essential for the enzyme–nucleotide interaction (Ehrlich & Colman, 1978; Mas & Colman, 1985), suggesting that any potential affinity label for this enzyme retain the 2′-phosphate.

Affinity labeling of the coenzyme binding site of $NADP^+$-dependent isocitrate dehydrogenase has previously

† This work was supported by USPHS Grant DK 39075.

0006-2960/87/0426-6858$01.50/0